

## Effects of imperfect spatial resolution on measurements of wall-bounded turbulent shear flows

By ARNE V. JOHANSSON AND P. HENRIK ALFREDSSON

Department of Mechanics, The Royal Institute of Technology, S-100 44 Stockholm, Sweden

(Received 13 September 1982 and in revised form 5 July 1983)

The effects of imperfect spatial resolution on hot-film and hot-wire measurements of wall-bounded turbulent shear flows were studied. Two hot-film probes of different length were used for measurements of fully developed turbulent channel flow in a water tunnel. In the near-wall region significant effects of spanwise spatial averaging due to finite probe size were found for a probe 32 viscous units long. The maximum turbulence intensity attained a 10% lower value than that for a probe about half as long, and the zero-crossing of the skewness factor was shifted away from the wall. This could be attributed to spatial averaging of narrow low-speed regions. Results for different Reynolds numbers, but with the same sensor length in viscous units, showed that Reynolds-number effects are small, and that much of the reported discrepancies for turbulence measurements in the near-wall region can be ascribed to effects of imperfect spatial resolution. Also the number of events detected with the variable-interval time-averaging (VITA) technique was found to depend strongly on the sensor length, especially for events with short duration.

---

### 1. Introduction

When measurements are carried out with hot wires or hot films the velocity measured by the probe will be a spatial average† along the sensor. Zarič (1972) and Coles (1978) compiled data from a large number of studies of wall-bounded turbulent shear flows and found large differences in the measured turbulence intensity in the near-wall region. These differences cannot be solely attributed to Reynolds-number effects. Since normally the length of the sensor cannot be considered small compared with the smallest scales of the turbulence, spanwise spatial averaging could be expected to influence the measurements. This is especially accentuated for high-Reynolds-number flows.

The effects of imperfect spatial resolution on measured turbulence intensity and (velocity) spectra have been studied theoretically by e.g. Frenkiel (1949, 1954), Corrsin & Kovasznay (1949) and Uberoi & Kovasznay (1953). The latter study was extended by Wyngaard (1968), who also made comparisons with experimental data for nearly isotropic turbulence in a curved mixing layer. The spatial resolution problem for hot wires has also been addressed by Bremhorst (1972) and Roberts (1973). Wyngaard (1969, 1971) treated the corresponding problem for various types of sensors such as a vorticity meter and a temperature sensor. The applicability of the above results to wall-bounded turbulent shear flows is, however, limited.

† Actually this is a weighted average owing to effects of non-uniform temperature distribution. If the velocity variation along the sensor is large the nonlinearity of the relation for the convective heat loss may also influence the averaging.

The visual studies of turbulent boundary layers by Kline *et al.* (1967) and Kim, Kline & Reynolds (1971) have shown that elongated structures, with a typical spanwise scale of 10–30 viscous length units ( $l_*$ ) are present close to the wall. Corino & Brodkey (1969) used trace particles to study the wall region in turbulent pipe flow and found that violent ejections of small spanwise scale (about  $20l_*$ ) take place in the buffer region. The length of hot-wire and hot-film sensors used in studies of pipe, channel and boundary-layer flows usually ranges from a few  $l_*$  to around  $100l_*$ . For the larger probes one would hence expect significant effects of spatial averaging on measurements close to the wall.

Effects of imperfect spatial resolution have also been reported for measurements of turbulent wall-pressure fluctuations. Schewe (1979) carried out measurements in air with transducers of different diameters (ranging from  $19l_*$  to  $350l_*$ ). He found that the measured intensity decreases with increasing sensor size and that this trend was evident also in other published data (see also Corcos 1963; Willmarth 1975). Spectra showed less high-frequency content for the larger transducers, as would indeed be expected if the reduction in measured intensity is due to spatial averaging. Also the skewness and flatness factors of the wall-pressure fluctuations were affected, primarily because of attenuation of large-amplitude fluctuations.

Turbulence production in the near-wall region takes place, to a large extent, during intermittently occurring ‘violent’ events (‘bursting’ periods). Several methods have been devised to detect these events from measured turbulence signals. Distortion of velocity signals due to spanwise averaging may influence results obtained with such detection schemes. For instance, Blackwelder & Haritonidis (1980) found that the number of events detected with the VITA technique decreases when larger probes are used.

The purpose of the present study was to investigate probe-length effects on measurements of the streamwise velocity component in the near-wall region of wall-bounded turbulent shear flows. The experiments were carried out in a fully developed turbulent water-channel flow. A description of the flow facility and experimental procedures is given in §2. The effects of spatial averaging were investigated with the use of two hot-film probes of different size, but with the same length-to-diameter ratio. A major portion of the results presented in §3 pertains to a Reynolds number for which the probe lengths correspond to 14 and 32 viscous length units. Significant differences in the measured probability density distributions of the streamwise velocity (and its time derivative) were found for this case in the near-wall region. The effects on the detection of events with the VITA method were found to be largest for events with short duration.

## 2. Experimental procedure

The experiments were performed in the water tunnel at the Department of Mechanics, at the Royal Institute of Technology, Stockholm. The measurements were carried out 69 channel heights from the inlet of the 6 m long test section, which is made of Plexiglas and has a width of 400 mm and a height of 80 mm. At this position the flow is fully developed as shown by Johansson & Alfredsson (1981). Boundary-layer-type hot-film probes (DISA model R15 and TSI model 1261-10W) were used together with the DISA M01 anemometer system for the measurements of the streamwise velocity component. The length  $L$  of the sensing element is 1.25 mm for the DISA probe and 0.50 mm for the TSI probe. The diameters  $D$  are 0.070 mm and 0.025 mm respectively, and hence the  $L$ -to- $D$  ratio of both these probes is about 20.

For hot wires in air an  $L/D$  of about 200 is needed to keep the influence of parasitic cooling by the prongs negligible. This effect is, however, much less severe for hot films in liquids, as pointed out by Blackwelder (1981).

For hot-film measurements it is of utmost importance to use clean water of constant temperature. A filtering and temperature-control system was employed for this purpose. During the experiments, the water temperature could thereby be kept constant to within  $\pm 0.03$  °C. The channel centreline velocity was measured before and after each run to check that no drift due to contamination of the hot-film probe had occurred during the measurements. If the measured velocity had changed by more than 2% the run was discarded. The absolute distance from the wall could be determined within about 0.03 mm.

The hot-film probes were calibrated in a submerged water jet. The calibration procedure was the same as used by Johansson & Alfredsson (1982), and the calibration curve could be matched to the data points with an error of less than 2% (in velocity). For each measurement point, 230 000 samples of the anemometer output signal were collected (after subtracting a d.c. voltage) through the 12 bit A/D converter of a DEC MINC system (PDP 11/23), and stored on a floppy disc. The time between consecutive samples was chosen as about half the viscous timescale.

Poor frequency response of the anemometer system may have an attenuating effect on the contribution to the turbulence signal from small-scale fluctuations. As the aim of this study was to investigate effects of spatial averaging due to finite probe size, one has to make sure that the results are not obscured by such an effect. A frequency limit of roughly 15 kHz was estimated both for the DISA and the TSI probes from the square-wave test. The interpretation of the square-wave test result for hot-film probes is, however, a more complicated matter than for hot wires, as pointed out by Freymuth & Fingerson (1977) and Freymuth (1978). To get a reliable check of the frequency response, measurements were carried out in the same (turbulent) flow with the hot-film probe and a hot-wire probe (DISA P15). The probes were placed (one at a time) at the same position in the turbulent outer part of the jet in the hot-film calibration apparatus. A filtering system kept the water free of particles to the extent that the hot wire could be run for long periods of time (several hours) without being damaged. A slow drift due to electrolysis of the unisolated hot wire is, however, unavoidable in this set-up. This drift does not significantly affect the power spectrum of the hot-wire signal at high frequencies. The frequency limit of the hot wire was estimated from the square-wave test to be about 20 kHz. Power spectra from the jet of the (non-linearized) signals measured with the hot wire and a DISA (R15) hot-film probe are shown in figure 1. The two probes have the same sensing length and were run at the same overheat (16 °C). The spectra collapse well up to at least 600 Hz, above which very little energy is found for the flows studied here.

Heat conduction to the wall often causes severe problems for hot-wire measurements close to the wall in air flows. Corrections of such data have been suggested e.g. by Wills (1962) and Bhatia, Durst & Jovanovic (1982). In the latter investigation it was shown that the effects can be kept very small by using a non-conducting wall material. A similar situation prevails for hot-film measurements in water flows over e.g. a Plexiglas surface. It is seen in figure 4 of Johansson & Alfredsson (1982) that the linear velocity distribution in the viscous sublayer can be well reproduced, which implies that effects of heat conduction to the wall are negligible in the experimental set-up used here.

Results concerning the effects of spatial averaging on the detection of events (or 'bursts') with the VITA-technique are presented in §3. With this technique,

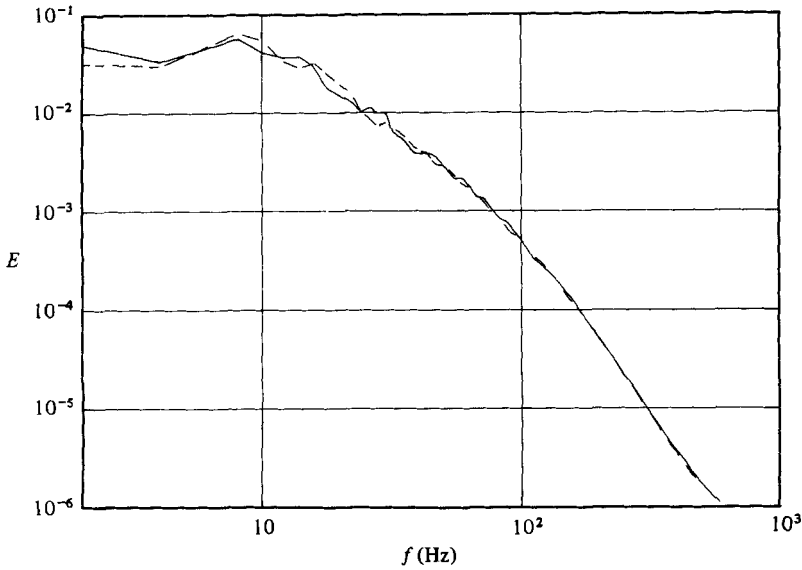


FIGURE 1. Power spectra from the outer region of a turbulent jet, obtained with the (DISA R15) hot-film probe (---) and with a (DISA P15) hot-wire probe (—). The overheat is 16 °C and the jet velocity is 0.5 m/s ( $E$  is the normalized energy density).

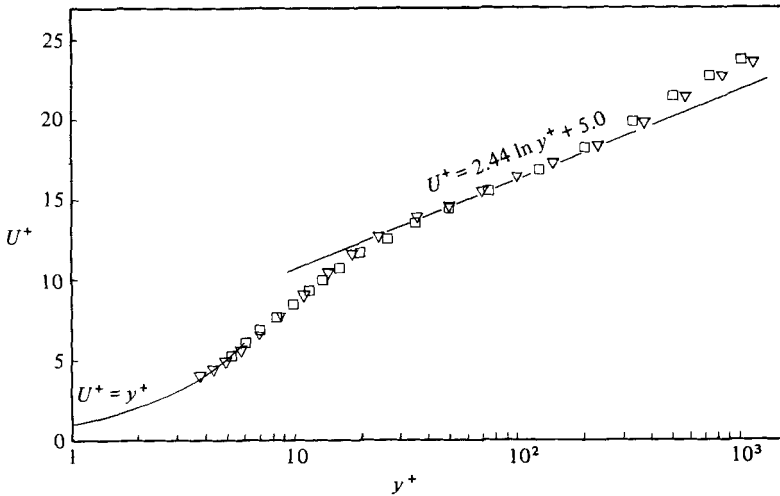


FIGURE 2. Mean-velocity distributions:  $\nabla$ ,  $Re = 54300$ ,  $L^+ = 14$ ;  $\square$ ,  $Re = 48900$ ,  $L^+ = 32$ .

developed by Blackwelder & Kaplan (1976), use is made of the intermittent character of the short-time variance of the streamwise velocity to detect events associated with the turbulence production. It is assumed that peaks in the short-time variance signal, defined as

$$\text{var}(t, T) = \frac{1}{T} \int_{t-\frac{1}{2}T}^{t+\frac{1}{2}T} u^2(s) ds - \left( \frac{1}{T} \int_{t-\frac{1}{2}T}^{t+\frac{1}{2}T} u(s) ds \right)^2,$$

correspond to such events. Two different types of event are detected, associated with an increase (accelerations) or a decrease (retardations) in the velocity at the detection

time. When the averaging time  $T$  becomes large the right-hand side tends to  $u_{\text{rms}}^2$ . An event is considered to occur when the short-time variance exceeds  $ku_{\text{rms}}^2$ , where  $k$  is a chosen threshold level. As was demonstrated by Johansson & Alfredsson (1982), there is a close relation between the mean duration of the detected events and the averaging time.

### 3. Results

A major portion of the results presented in the following was obtained from experiments carried out with the two probes described in the previous section, at a Reynolds number  $Re$  (based on channel height  $2b$  and centreline velocity  $U_{\text{CL}}$ ) of about 50000. At this Reynolds number the probe lengths correspond to 14 and  $32l_*$ . In the light of the findings from the visual studies of e.g. Kim *et al.* (1971) concerning the spanwise scale of low-speed regions, this is a suitable choice of probe lengths for an investigation of effects of spanwise spatial averaging on measurements of near-wall turbulence. The Kolmogorov lengthscale  $\eta$  is often used as an estimate of the smallest scale of the turbulence. For this case it can be estimated from the mean turbulent dissipation to be approximately  $3l_*$ . The  $L/\eta$  ratio for the larger probe falls in the range where significant effects of spatial averaging were found by Wyngaard (1968) for high-frequency components of nearly isotropic turbulence in a curved mixing layer. To establish the relative importance of the effects of spatial averaging as compared to Reynolds-number effects, measurements were also carried out with the smaller probe at a high Reynolds number ( $Re = 129000$ ). This was chosen such that the sensor length in viscous units equals that of the larger probe for the lower-Reynolds-number case described above.

The mean-velocity distributions at  $Re \approx 50000$  measured with the two probes are seen in figure 2 to agree well. The friction velocity  $u_\tau$  was determined from the best fit to the logarithmic velocity law

$$U^+ = \frac{1}{\kappa} \ln y^+ + B$$

( $U^+ = U/u_\tau$  and  $y^+ = y/l_*$ ) with the standard values  $\kappa = 0.41$  and  $B = 5.0$  (see Coles 1968). A  $U_{\text{CL}}/u_\tau$  ratio of 23.5 was found suitable for both cases in figure 2, whereas a ratio of 25.0 was found for the high-Reynolds-number case.

A comparison between results obtained with the two different probes, for the distributions of  $u_{\text{rms}}$ , skewness and flatness is presented in figure 3. The effects of spatial averaging on the measured turbulence intensity are clearly seen. The maximum intensity, which is found at about  $y^+ = 15$ , is 10% lower for the larger probe. Somewhat closer to the wall the differences are even larger, whereas, above  $y^+ = 30$ , the data collapse onto one curve. The differences indicate significant contributions to the turbulence intensity from spanwise lengthscales smaller than  $30l_*$  in the buffer region (around  $y^+ = 10$ ), and, as expected, that the spanwise scales increase with increasing distance from the wall. It is interesting to note that the high-Reynolds-number data (for which  $L^+ = 33$ ) differ little from the data obtained at  $Re \approx 50000$  with the larger probe (i.e. with  $L^+ = 32$ ). This is true also for the higher moments (figures 3*b*, *c*), and indicates that Reynolds-number effects are small for moments of  $u$  in the near-wall region, at least when one compares measurements on the laboratory scale.

Effects of spatial averaging on the skewness and flatness factors are observed somewhat further out than the effects on turbulence intensity. When interpreting

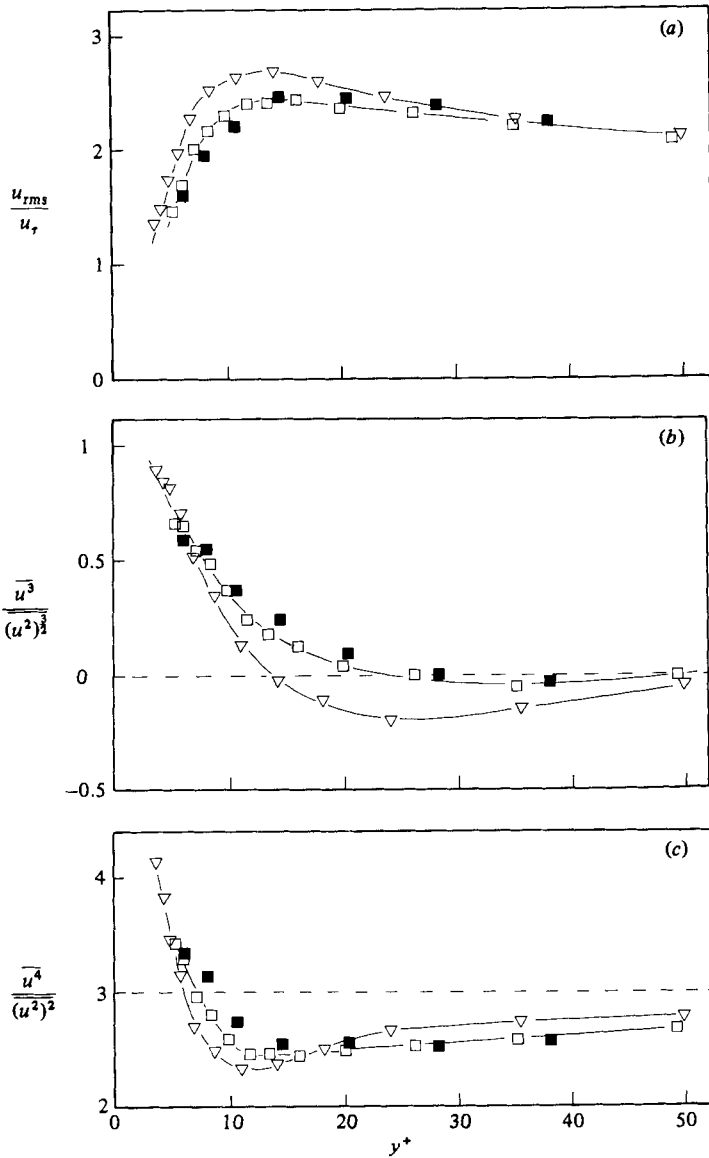


FIGURE 3. Distributions of (a) turbulence intensity, (b) skewness factor and (c) flatness factor, in the near-wall region, for a moderate Reynolds number ( $\approx 50000$ ):  $\nabla$ ,  $L^+ = 14$ ;  $\square$ ,  $L^+ = 32$ ; and a high Reynolds number (129000):  $\blacksquare$ ,  $L^+ = 33$ .

these results one should, however, bear in mind the normalization with  $u_{rms}^3$  and  $u_{rms}^4$  respectively (since  $u_{rms}$  itself is affected by spatial averaging). Notable is that the skewness factor has a zero-crossing further from the wall when obtained from measurements with the larger probe. An equivalent effect of imperfect spatial resolution was also observed by Moin & Kim (1982) in a numerical investigation (large-eddy simulation) of turbulent channel flow. The zero-crossing in their case occurred at about  $y^+ = 50$ . Also the maximum turbulence intensity occurred somewhat farther from the wall with a value lower than that obtained in experimental studies.

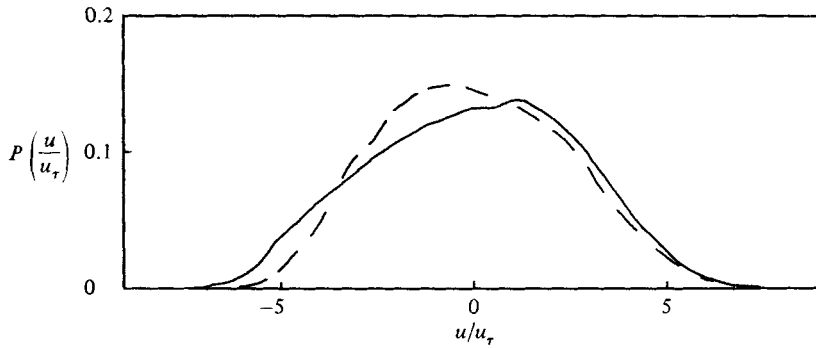


FIGURE 4. Probability density distributions of  $u$  at  $y^+ \approx 14$ ,  $Re \approx 50000$ :  
 —,  $L^+ = 14$ ; ---,  $L^+ = 32$ .

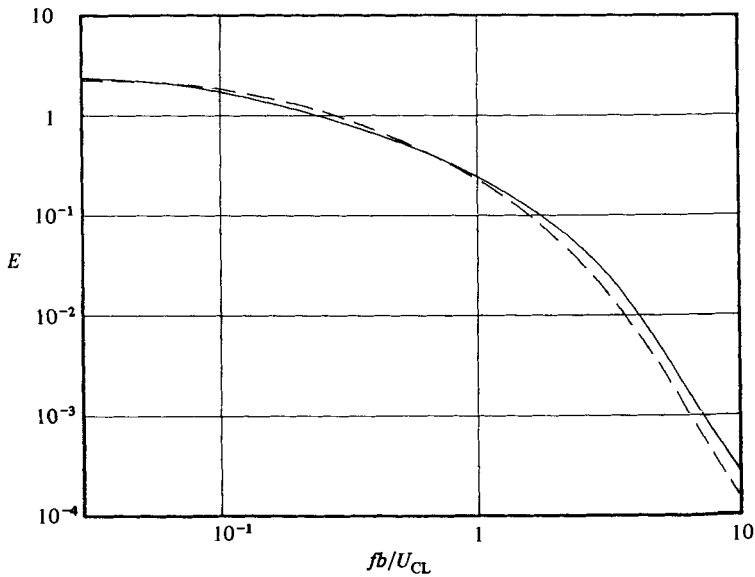


FIGURE 5. Power spectra of the streamwise velocity fluctuations at  $y^+ \approx 14$ ,  $Re \approx 50000$ :  
 —,  $L^+ = 14$ ; ---,  $L^+ = 32$ .

The higher value of the skewness factor (figure 3*b*) in the buffer region as measured with the larger probe can mainly be ascribed to spatial averaging of low-velocity regions of small spanwise extent. This leads to attenuation of large negative velocity fluctuations, as can be seen (figure 4) from the probability density distributions of  $u$  at  $y^+ = 14$ , for the two measurements at  $Re \approx 50000$ . The corresponding power spectra for this position are shown in figure 5. The difference in turbulence intensity is about 10%, and it can be seen that this is mainly due to the attenuation of high-frequency components ( $fb/U_{CL} > 1$ ). The highest frequency in figure 5 (viz.  $fb/U_{CL} = 10$ ) corresponds to a non-dimensional wavenumber  $k\eta$  of about 0.5. According to the results of Wyngaard (1968) for isotropic turbulence, the larger probe would measure an energy density about 40% lower than that for the smaller probe, at this wavenumber. This is in fair agreement with the results in figure 5. However, the predicted attenuation at lower frequencies, such as  $fb/U_{CL} = 2$ , is too small.

A distinct feature of the fluctuating streamwise velocity signal, in the near-wall

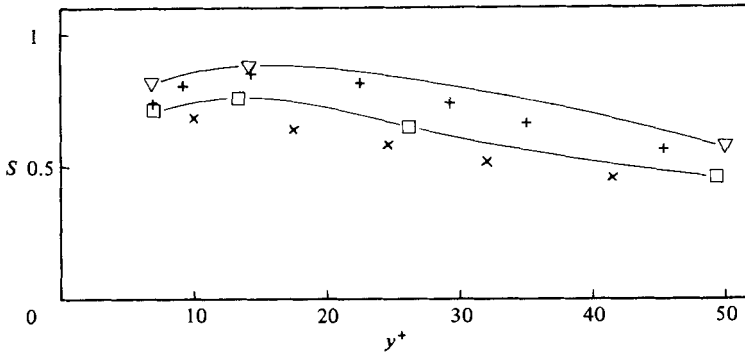


FIGURE 6. Distribution of the skewness of  $\partial u/\partial t$  in the near-wall region for  $Re \approx 50\,000$ :  $\nabla$ ,  $L^+ = 14$ ;  $\square$ ,  $L^+ = 32$ ; and data of Comte-Bellot (1965):  $+$ ,  $L^+ = 13$ ;  $Re = 125\,000$ ;  $\times$ ,  $L^+ = 36$ ,  $Re = 506\,000$ .

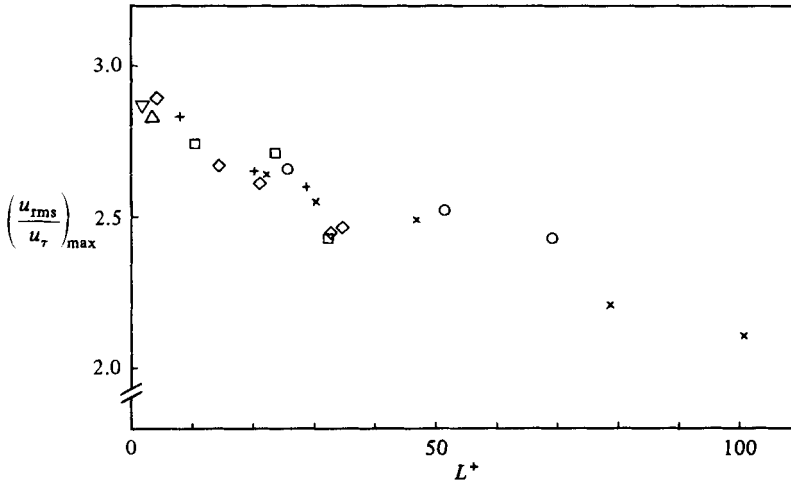


FIGURE 7. The maximum turbulence intensity as function of the probe length in viscous units. The symbols are explained in table 1.

region, is the predominance of strong accelerations. A possible interpretation is that they are associated with the passage (across the probe) of internal shear layers. This characteristic of the  $u$ -signal can also be seen from conditional averages constructed with the VITA detection scheme of Blackwelder & Kaplan (1976) or with the pattern-recognition technique of Wallace, Brodkey & Eckelmann (1977). It results in a high positive value of the skewness  $S$  of the time derivative of  $u$ . This quantity is also of interest in studies of isotropic turbulence (see e.g. Frenkiel & Klebanoff 1971). The skewness  $S$  is quite sensitive to effects of spatial averaging (figure 6), and the effects extend further out from the wall than is the case for the moments of  $u$ . Data of Comte-Bellot (1965), for comparable probe lengths, are included in figure 6. The agreement is reasonably good between the two sets of data, although the highest Reynolds number of Comte-Bellot is considerably higher than those for the present cases. Also Wallace *et al.* (1977) measured  $S$  in a turbulent channel flow, at a low Reynolds number. The probe is in their case extremely small in terms of viscous units, and the values of  $S$  in the near-wall region are somewhat higher than the present

Experiment	Type of flow	Linearization	Symbol
Eckelmann (1974)	Oil channel	Analog	▽
Kreplin (1976)	Oil channel	Analog	△
Hussain & Reynolds (1970)	Air channel	Analog	○
Johansson & Alfredsson (1982)	Water channel	Digital	□
Karlsson (1980)	Air boundary layer	Digital	×
Purtell <i>et al.</i> (1981)	Air boundary layer	Analog	+
Present results	Water channel	Digital	◇

TABLE 1. Investigations included in figure 7

results for  $L^+ = 14$ . Also the flatness and other moments are affected by spatial averaging. The reduction of the r.m.s. value of  $\partial u/\partial t$  was found to be somewhat larger than for the turbulence intensity.

Early experimental studies of turbulence, such as those of Laufer (1951, 1954) and Klebanoff (1955), were carried out with constant-current anemometry. Today one is confident (see e.g. Comte-Bellot 1976) that constant-current operation leads to unwanted loss of accuracy at turbulence levels higher than about 5%. It is notable, however, that nonlinear effects are less severe for 'even' than for 'odd' moments (as pointed out by one of the referees). It is also necessary to use linearization (analog or digital) to get reliable results. In figure 7 we have compiled data on the maximum turbulence intensity from measurements of channel and boundary-layer flows, and plotted them versus the probe length in viscous units.† All data in figure 7 were obtained with constant-temperature anemometry and with linearization (no corrections applied for cooling by the velocity component along the sensor or other higher-order effects). However, the abovementioned constant-current data are also in reasonable agreement with the results presented here. Despite the differences in flow situation between the studies, listed in table 1, there is a clear trend in the data. A decrease of about 28% is observed over the presented range of sensor lengths, i.e. up to  $100l_*$ .

For the bulk of the data in figure 7, the friction velocity was determined from the condition of best fit to the logarithmic velocity law with  $\kappa = 0.41$  and  $B = 5.0$ . However, for the Göttingen data (Eckelmann 1974; Kreplin 1976) and the present data for a low Reynolds number (14000),  $u_\tau$  could be determined directly from the linear velocity distribution in the viscous sublayer. The resulting  $B$ -values for these cases are considerably higher than 5.0. A fit to the log law with  $B = 5.0$  for such cases would yield a higher value of  $u_\tau$ , and hence a more plateau-like character, at small values of  $L^+$ , of the correlation in figure 7. The boundary-layer data of Karlsson (1980) were obtained with  $u_\tau$  from a log-law fit (with  $B = 5.0$ ). However, he simultaneously measured the skin friction with a floating-balance device, which gave somewhat smaller values of  $u_\tau$  (up to 10% difference) for low Reynolds numbers.‡ This is consistent with the abovementioned findings for channel flow, and indicates that  $B$  may have a somewhat larger value than 5.0 at low Reynolds numbers. Such a trend is evident also in the data of Murlis, Tsai & Bradshaw (1982), although the authors

† One should be aware of the fact that the effective length of hot wires may be somewhat smaller than the physical length because of the non-uniform temperature distribution caused by cooling by the prongs.

‡ Low Reynolds numbers correspond to small  $L^+$  values in his case since the physical wire length was constant.

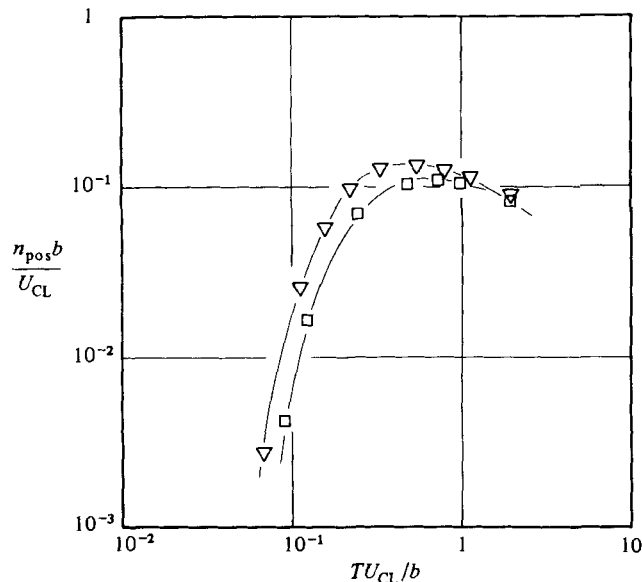


FIGURE 8. The frequency of occurrence of VITA events corresponding to accelerations as function of the integration time. The events are detected with  $k = 1.0$  at  $y^+ \approx 14$ ,  $Re \approx 50000$ :  $\nabla$ ,  $L^+ = 14$ ;  $\square$ ,  $L^+ = 32$ .

of that paper ascribe it to measurement errors. This issue, which has some implications for studies of low-Reynolds-number flows, does not yet seem to be completely settled (see also Purtell, Klebanoff & Buckley 1981).

Also the detection of events (or 'bursts') depends on the spatial resolution of the probe (independent of the detection scheme). The VITA technique singles out events with a duration which is roughly the same as the averaging time  $T$  used (see Johansson & Alfredsson 1982). The distribution of timescales of the events can then be inferred from plots of frequency of occurrence as function of  $T$ . Blackwelder & Haritonidis (1980) studied the 'bursting frequency' in a turbulent boundary layer and found that the number of events detected per unit time with the VITA method decreases with increasing probe length, for an average time of  $10t_*$  ( $t_*$  is the viscous timescale).

The frequency of occurrence of events detected, at  $y^+ \approx 14$  ( $Re \approx 50000$ ), with the two probes is shown in figure 8 as a function of the averaging time (the number of events detected per unit time, corresponding to accelerations, is denoted by  $n_{\text{pos}}$ ). Large differences are seen for short averaging times, corresponding to frequencies where the attenuation in the power spectrum for the larger probe is found in figure 5. For an averaging time of 0.1 in outer units (corresponding to approximately  $5t_*$ ) about three times as many events are detected with the smaller probe. However, for large averaging times ( $TU_{\text{CL}}/b > 1$ ) the data collapse onto one curve. A threshold level of 1.0 was used in this case, but similar results were obtained also for other threshold levels. The differences are indeed somewhat larger than what is indicated by figure 8, since events, detected with the same threshold level, have a larger mean amplitude (owing to the larger value of  $u_{\text{rms}}$ ) for the small-probe case. It should be noted that the results of figure 8 are independent of the scaling used, since the Reynolds numbers are about the same for the two measurements.

The spatial-averaging effects on moments of the time derivative of  $u$ , and the detection of events extend somewhat further out from the wall than those on moments of  $u$ , but all are practically negligible in the outer flow region.

#### 4. Discussion and conclusions

As was shown in §3, there is a strong correlation between the measured value of the maximum turbulence intensity and the probe length (in viscous units). The maximum turbulence intensity (figure 7) decreased from about  $2.9u_\tau$  for the smallest probes to  $2.1u_\tau$  for a probe  $100l_*$  long. This conclusion is based on constant-temperature hot-wire (film) data compiled from various studies (including the present) of channel and boundary-layer flows, and agrees reasonably well also with earlier data obtained with constant-current anemometry. The reduction (28 %) is comparable to the results of Schewe (1979) for the r.m.s. value of wall-pressure fluctuations measured with sensors of different diameters at a fixed Reynolds number. One could of course argue that there is a similar trend in the correlation between the maximum turbulence intensity and the Reynolds number. This correlation is, however, much weaker than that seen in figure 7. As shown in figure 3(a), significant differences (10 %) in the measured turbulence intensity were found for different sensor lengths at about the same Reynolds number, whereas measurements at different Reynolds numbers, but with the same sensor length (in viscous units) agree well. Much of the discrepancies between different studies concerning the turbulence intensity in the near-wall region (see Zarič 1972; Coles 1978) therefore appears to be attributable primarily to imperfect spatial resolution, and not so much to Reynolds-number effects.

For studies of wall-bounded shear turbulence it is in general of great importance to know the friction velocity with good accuracy. The correlation between  $u_{\text{rms}}/u_\tau$  and the sensor length in viscous units (figure 7) provides a means of checking the value of  $u_\tau$  obtained from e.g. a Clauser plot, although more accurate data are needed to complete the picture.

Considerable attenuation of large negative velocity fluctuations were found in the buffer region, for a probe  $32l_*$  long (figure 4). This may be seen as an indirect confirmation of the observed small spanwise lengthscales of ejections (Corino & Brodkey 1969; Kim *et al.* 1971). Sweeps ( $u > 0$ ,  $v < 0$ ) have been observed to have larger spanwise lengthscales, and should therefore be less affected by spatial averaging, which indeed is supported by the results in figure 4. The contributions to the Reynolds stress from ejections and sweeps are equal at around  $y^+ = 15$  (see Brodkey, Wallace & Eckelmann 1974). Closer to the wall the sweeps dominate and *vice versa*. Also the zero-crossing of the skewness factor is located at about  $y^+ = 15$ . The sweeps and ejections give contributions of opposite signs to the skewness (positive and negative respectively). Now, when measurements are taken with a large probe, it is primarily the ejections that are subject to spatial averaging. This leads to a shift of the zero-crossing away from the wall and, in general, to an increase of the skewness factor (of  $u$ ).

In the region where large probe-size effects on turbulence intensity and skewness are seen in figure 3, also the detection of events with the VITA method was found to be affected by spatial averaging (figure 8). These events can, in general, be characterized as localized rapid accelerations of the flow. With large probes these are averaged out, which also leads to a reduction of the skewness of  $\partial u/\partial t$  (figure 6). Blackwelder & Haritonidis (1980) found a significant decrease in the number of detected VITA events (with  $T = 10t_*$ ) for probes longer than about  $20l_*$ , and suggested a correction factor that is a function of  $L^+$  only. Applied to the cases in figure 8, this correction factor gives a result that is of the correct order of magnitude for  $T/t_* \approx 10$ . However, this factor contains no dependence on the averaging time and hence cannot explain the trend seen in figure 8. It seems to be in agreement with physical intuition, and with the spectral results in figure 5, that the effects of spatial

averaging should be stronger for short averaging times, since  $T$  is strongly coupled to the duration of the events. It is also of vital importance to be aware of the effects of spatial averaging on the detection of events, when trying to establish a scaling law for their frequency of occurrence (cf. 'bursting' frequency) from results for different Reynolds numbers.

The work reported here is part of a research program sponsored by the Swedish Maritime Research Centre (SSPA). We gratefully acknowledge this support. We also want to thank Professors Märten Landahl and Fritz Bark for fruitful discussions, and the referees for constructive criticism.

## REFERENCES

- BHATIA, J. C., DURST, F. & JOVANOVIĆ, J. 1982 *J. Fluid Mech.* **122**, 411.
- BLACKWELDER, R. F. 1981 In *Methods of Experimental Physics*, vol. 18A (ed. R. J. Emrich), p. 273.
- BLACKWELDER, R. F. & HARITONIDIS, J. H. 1980 *Bull. Am. Phys. Soc.* **25**, 1094.
- BLACKWELDER, R. F. & KAPLAN, R. E. 1976 *J. Fluid Mech.* **76**, 89.
- BREMHORST, K. 1972 In *Trans. on Instrumentation and Measurement*, IM-21, 244.
- BRODKEY, R. S., WALLACE, J. M. & ECKELMANN, H. 1974 *J. Fluid Mech.* **63**, 209.
- COLES, D. E. 1968 In *Proc. AFOSR-IFP-Stanford Conf. on Computation of Turbulent Boundary Layers* (ed. D. E. Coles & E. A. Hirst), vol. 2, p. 1.
- COLES, D. E. 1978 In *Proc. Workshop on Coherent Structures of Turbulent Boundary Layers, Lehigh Univ.* (ed. C. R. Smith & D. E. Abbott), p. 462.
- COMTE-BELLOT, G. 1965 *Publ. Sci. Tech. de l'Air* no. 419.
- COMTE-BELLOT, G. 1976 *Ann. Rev. Fluid Mech.* **8**, 209.
- CORCOS, G. M. 1963 *J. Acoust. Soc. Am.* **35**, 192.
- CORINO, E. R. & BRODKEY, R. S. 1969 *J. Fluid Mech.* **37**, 1.
- CORRSIN, S. & KOVASZNYI, L. S. G. 1949 *Phys. Rev.* **75**, 1954.
- ECKELMANN, H. 1974 *J. Fluid Mech.* **65**, 439.
- FRENKIEL, F. N. 1949 *Phys. Rev.* **75**, 1263.
- FRENKIEL, F. N. 1954 *Aero. Q.* **5**, 1.
- FRENKIEL, F. N. & KLEBANOFF, P. S. 1971 *J. Fluid Mech.* **48**, 183.
- FREYMUTH, P. 1978 *TSI Q.* **4** (2), 2.
- FREYMUTH, P. & FINGERSON, L. M. 1977 *TSI Q.* **3** (4), 5.
- HUSSAIN, A. K. M. F. & REYNOLDS, W. C. 1970 *Dept Mech. Engng, Stanford Univ., Rep.* FM-6.
- JOHANSSON, A. V. & ALFREDSSON, P. H. 1981 *R. Inst. Tech., Stockholm, Rep.* TRITA-MEK-81-04 (ISSN 0348-467 X).
- JOHANSSON, A. V. & ALFREDSSON, P. H. 1982 *J. Fluid Mech.* **122**, 295.
- KARLSSON, R. 1980 *Dept. Appl. Thermo and Fluid Dynamics, Chalmers Univ. Tech., Gothenburg, Doctoral thesis.*
- KIM, H. T., KLINE, S. J. & REYNOLDS, W. C. 1971 *J. Fluid Mech.* **50**, 133.
- KLEBANOFF, P. S. 1955 *NACA Rep.* 1247.
- KLINE, S. J., REYNOLDS, W. C., SCHRAUB, F. A. & RUNSTADLER, P. W. 1967 *J. Fluid Mech.* **30**, 741.
- KREPLIN, H.-P., 1976 *Mitt. MPI f. Strömungsforschung u. der AVA, Göttingen*, no. 63.
- LAUFER, J. 1951 *NACA Rep.* 1053.
- LAUFER, J. 1954 *NACA Rep.* 1174.
- MOIN, P. & KIM, J. 1982 *J. Fluid Mech.* **118**, 341.

- MURLIS, J., TSAI, H. M. & BRADSHAW, P. 1982 *J. Fluid Mech.* **122**, 13.
- PURTELL, L. P., KLEBANOFF, P. S. & BUCKLEY, F. T. 1981 *Phys. Fluids* **24**, 802.
- ROBERTS, J. B. 1973 *Aero. J.* **77**, 406.
- SCHEWE, G. 1979 *Mitt. MPI f. Strömungsforschung u. der AVA, Göttingen*, no. 68A, ISSN 0374-1257.
- UBEROI, M. S. & KOVASZNY, L. S. G. 1953 *Q. Appl. Maths* **10**, 375.
- WALLACE, J. M., BRODKEY, R. S. & ECKELMANN, H. 1977 *J. Fluid Mech.* **83**, 673.
- WILLMARTH, W. W. 1975 *Ann. Rev. Fluid Mech.* **7**, 13.
- WILLS, J. A. B. 1962 *J. Fluid Mech.* **12**, 388.
- WYNGAARD, J. C. 1968 *J. Phys. E: Sci. Instrum.* **1**, 1105.
- WYNGAARD, J. C. 1969 *J. Phys. E: Sci. Instrum.* **2**, 983.
- WYNGAARD, J. C. 1971 *Phys. Fluids* **14**, 2052.
- ZARIČ, Z. 1972 *Adv. Heat Transfer* **8**, 285.